Contact-less Monitoring of the Major Blood Vessels Supplying Head and Brain (Carotid Arteries)

Shahrzad Jalali Mazlouman, Alireza Mahanfar, and Bozena Kaminska
CiBER Lab, School of Engineering Science
Simon Fraser University
8888 University Drive, V5A 1S6, Burnaby, BC, Canada
{sja53,nima_mahanfar,Kaminska}@sfu.ca

ABSTRACT

In this paper, the development of a system for measuring heart-rate and blood flow in the Carotid arteries is reported that require no physically connecting electrodes or other sensors to the body. The measurement system was implemented to simultaneously monitor the Carotid arteries and heart rate in order to get more valid information for detection and diagnosis of cardiovascular disease. The designed system is based on the Microwave Doppler radar concept with frequency of 2.4GHz and at the distance of up to 3 cm and is capable of detecting the vibrations of the Carotid arteries, without any contact with the person's body. The basic theory, a feasibility analysis and modeling, and preliminary measurement results of our basic Carotid arteries monitoring setup are presented.
Keywords: Cerebral blood flow, Carotid arteries, health monitor, contact less, Microwave Doppler-based radar.

1 INTRODUCTION

Ultrasonography has become an important diagnostic method in the area of cardiovascular and cerebrovascular diseases [1]. Doppler ultrasound devices are able to provide information on blood flow velocity in a large number of arteries and veins. Examples include the Carotid and major cerebral arteries in association with the prediction and treatment of stroke. When coupled with two and three-dimensional imaging, factors such as plaque build-up and stenosis can be measured. Many applications have been suggested; for example, in congenital heart surgery, the evaluation of cerebral blood flow variations during cardiopulmonary bypass (CPB) can be useful. Ultrasound technology has also led to the ability for real time dynamic imaging of cardiac function in two and three dimensions.

A typical example of the application of ultrasonography is the use of Transcranial Doppler Ultrasound (TCD) to measure blood flow in cerebral vessels. However, cerebral measurements can only be made from limited regions where the skull is thin enough to allow penetration of the ultrasound beam. With aging, the thickness of the skull increases making measurements more difficult.

Despite its advantages such as being a non-invasive and relatively inexpensive imaging method, Ultrasonography has the disadvantage of requiring physical contact with the patient as well as minimal presence of underlying bone that impedes transmission of the ultrasound beam.

Recent developments in our laboratories indicate that microwave Doppler radar can be used to assess blood flow velocity in a wide range of blood vessels within the human body. An advantage of using microwave radar is the ability to choose the illuminating radar frequency depending on the application. Adjustment of frequency allows for measurements over a range of depths and for penetration of the skull for cerebrovascular measurements. The use of Doppler radar is similar to that of Doppler ultrasound but with the extra feature of vascular and neurovascular diseases diagnosis capability. Our initial experiments are very encouraging and suggest that blood flow dynamics measured by non-contact radar are comparable to and likely excel that obtained by ultrasound imaging.

In this paper, the design of a system for measuring Carotid arteries blood flow is discussed that requires no physically connecting electrodes or other sensors to the body. The measurement system is implemented to simultaneously monitor the Carotid arteries blood flow and the heart rate in order to get more valid information for detection and diagnosis of cardiovascular disease. The designed apparatus is based on Doppler radar with a centre frequency of 2.45 GHz, and is capable of detecting the blood flow rate in the Carotid Arteries, without any contact with the person's body, at a distance of up to 3 cm.

The structure of this paper is as follows. In Section 2, the developed Doppler radar system prototype is briefly introduced. In Section 3, a feasibility analysis is presented on the blood flow measurement of the Common Carotid artery in the neck and in the cerebral arteries under the skull using Doppler radar. This analysis is carried out by calculating the minimum required power to be propagated through a simplified linear model for typical body tissues involved in the measurement. Finally, Sections 4 and 5 are devoted to depiction of preliminary captured data, discussions, and conclusions.

2 THE DOPPLER RADAR SYSTEM

A block diagram of the Doppler radar-based apparatus is shown in Figure.1. As can be seen in this figure, the system is composed of an RF Doppler radar stage and a baseband signal processing stage. The radar stage is composed of a Microwave motion sensor based on Doppler radar. The motion sensor includes the transmitter and the receiver, as well as the propagating antennas in the same housing. The time delay between transmitted and received pulse also provides the opportunity for using a single antenna for send/receive and switching the path in send and receive cycle. This motion sensor transmits a continuous 2.45 GHz signal.

The reflected wave has almost the same shape as the transmitted, and includes a frequency shift proportional to the blood flow velocity. Therefore, down-conversion and filtering at the receiver side suppresses the 2.45 GHz carrier radar signal and leaves the Doppler shifted signal in the baseband for further processing in the baseband stage.

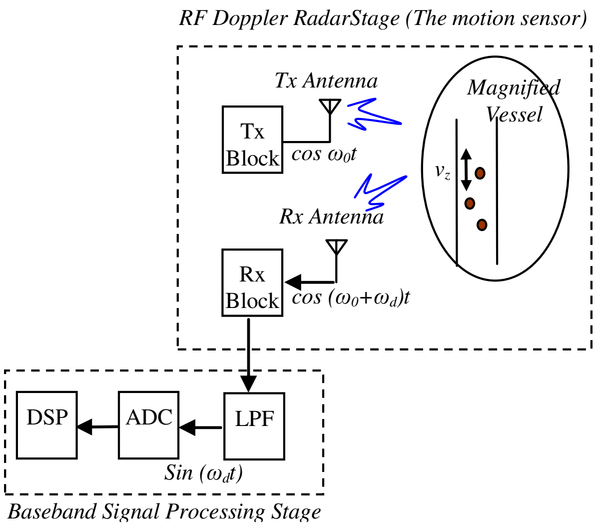

Figure 1: The radar system setup.

The baseband signal captured from the motion sensor is then bandpass-filtered, amplified, and converted into digital. As shown in Figure. 1, these blocks constitute the baseband signal processing stage that can be connected to a PC, or be implemented independently on a board. Digital signal processing techniques can be exploited to extract valuable data from the signal captured by the radar system.

This prototype has previously been proven to successfully monitor the cardiac vibration activity, including mechanical vibrations of the heart as recorded from the chest, i.e. the Meachanocardiograph (MCG), also called seismocardiograph, as well as the heart and respiration rate and heart rate variability (HRV) [2].

3 FEASIBILITY ANALYSIS

Several locations on the head can be used to examine the basal cerebral arteries, but the most reproducible and often used technique is to illuminate the middle cerebral artery (MCA) through the temporal bone window which is about 1 cm in front of the external auditory meatus and about 1–2 cm above the zygomatic arch. The Microwave beam is directed horizontally. The depth of the sample volume and beam angle is adjusted until the bifurcation of the MCA and the anterior cerebral artery (ACA) is reached (positive deflection toward the transducer from the MCA and a retrograde signal with a negative deflection from the ACA). A stable, clear, resting baseline at the beginning of the recordings is important to compare to later data, e g. during interventions such as pCO2 changes during hyperventilation or cardiovascular challenges such as orthostatic tolerance testing. Major cerebral arteries and the Common Carotid artery are shown in Figure 2.

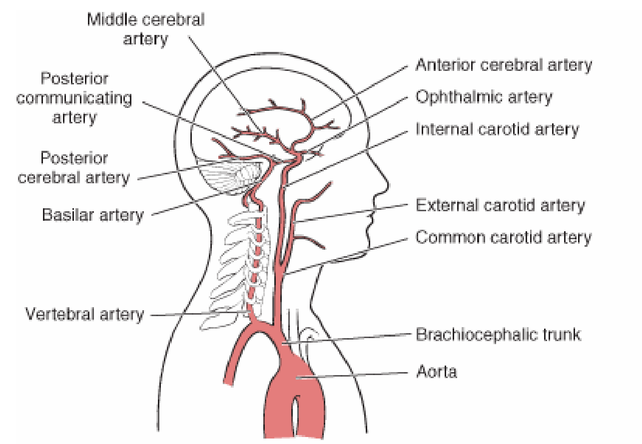

Figure 2: Major cerebral arteries, lateral view [©3].

A feasibility study of the Doppler radar measurement method is conducted using simple, yet conclusive, analysis and simulations. In this analysis, a simplified planar model is used for typical body tissue thicknesses involved for the measurement of the Common Carotid artery in the neck and in the cerebral arteries under the skull using Doppler radar.

Since the curvature of the neck and the head is negligible compared to the illuminated area by the microwave beam, the simplifying assumption of flat surface holds relatively valid for practical purposes. The model is shown in Figure 3. The thicknesses of the tissue layers, as well as their dielectric properties, i.e., permittivity and loss tangent, for the depicted model at the frequency of 2.45 GHz are presented in Table I.

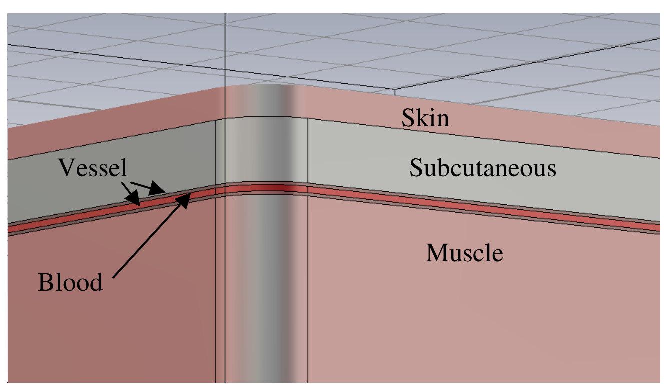

Figure 3: planar model used for power level calculations.

NSTI-Nanotech 2009, www.nsti.org, ISBN 978-1-4398-1783-4 Vol. 2, 2009

Table I. Thicknesses and Dielectric properties of the modeled tissue layers at the frequency of 2.45 GHz [4].

Layer	Tissue	Permittivity	Tanδ	Thickness
1	Skin	38.00	0.28	5mm
2	Subcutaneous	5.28	0.14	10mm
3	Blood Vessel	42.53	0.25	0.5mm
4	Blood	58.26	0.32	1mm

A continuous, 2.45 GHz wave is radiated through this tissue model. The radiated wave is assumed to be plane wave (TEM mode) thus the electric and magnetic field vectors are normal to each other and both normal to the direction of propagation.

Using this assumption, the propagation constant of layer *i*, can be written as [5]:

$$\gamma_i = j\omega\sqrt{\mu\varepsilon_i(1 - j\tan\delta_i)} \quad (1)$$

$$\alpha_i = \mathrm{Re}\{\gamma_i\} \quad (2)$$

Where μ is the permeability, ε_i is the permittivity of the tissue layer *i*, and ω is the angular frequency (in this case $2\pi\times 2.45$GHz). The real part of γ_i, α_i is the attenuation coefficient of tissue layer *i* (m^{-1}). The impedance of each layer *i* can be written as [5]:

$$Z_i = {j\omega\mu}/{\gamma_i} \quad (3)$$

Also, the transmission coefficient of TEM wave from layer *i* to layer *j*, T_{ij} and the reflection coefficient of the wave at the boundary between layers *i* and *j*, Γij can be written as[5]:

$$\Gamma_{ij} = \frac{Z_j - Z_i}{Z_j + Z_i} \quad (4)$$

$$T_{ij} = 1 - \left|\Gamma_{ij}\right| \quad (5)$$

The power in the forward path at point *x* of layer *I* can be written as:

$$P_I(x, f) = P(0)\exp(-\alpha_I(x - x_{I-1})) \prod_{i=1}^{I-1} T_{i,i-1}\exp(-\alpha_i(x_i - x_{i-1})) \quad (6)$$

where *P(0)* is the radiated power, and $P_I(x, f)$ is the power at point *x* within layer *I*. The return power $P_I^r(x, f)$ can be calculated in a similar manner:

$$P_I^r(x, f) = P_I(x_4, f).\Gamma_{3,4}.\exp(\alpha_I(x - x_I)) \prod_{i=I+1}^{3} T_{i,i-1}\exp(\alpha_i(x_{i-1} - x_i)) \quad (7)$$

The resulting power diagram is shown in figure 4. As can be seen in Figure 4, the overall attenuation of the wave for a two-way path through vessels is less than 35 dB. According to FCC part 15 regulations [6], the maximum conductive output power is 1W (30dBm) and the maximum allowed effective isotropic radiated power (EIRP) is 4W (i.e. 36dBm). Assuming a typical antenna with 6dBi gain, the maximum allowed power can be radiated. With 30dBm radiated power, the reflected power level, based on the diagram in Figure 4, will be around -5dBm. This level of received power is easily within the range of simplest detectors. For instance a typical schottky diode such as HSMS282 [7] can detect power levels as low as -40dBm.

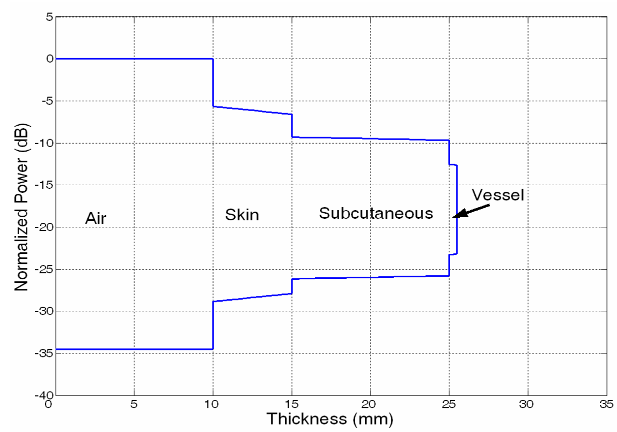

Figure 4: Normalized power diagram for planar model with TEM mode.

The same structure is modeled using commercially available Finite-Difference Time-Domain (FDTD) method. The results provide additional information about the power absorbed in different layers. As can be observed in Figure 5, the losses through the subcutaneous layer are smaller compared to the skin. A significant portion of the power is dissipated in the skin, and another part of it is dissipated in the blood vessel layer.

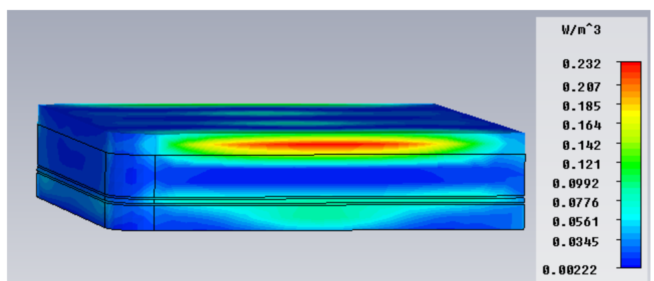

Figure 5: The power loss density in different tissue layers in the planar conceptual model. It can be seen that a significant portion of power is dissipated in the skin.

Another conclusion from the numerical analysis is the electric field strengths for an x-directed incident plane wave in different layers as shown in Figure 6. The electric field has a frequency selective behavior. This is mainly due to the high dielectric constants of the tissue layers that cause dielectric cavity resonance. Also, despite the pure linear polarization of the incident field, some cross-polarization components can be observed. These components are of special interest in polarimetric study and may contain important and useful information about tissue properties.

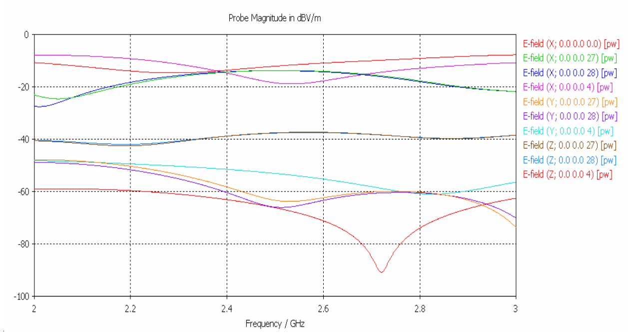

Figure 6: Electric field components at different locations.

Another concern for use of this method is health and safety issues. The Simulated SAR values using the FDTD method show values below 0.2W/Kg (1g sampling) that is well below the 1.6W/Kg SAR limit [6].

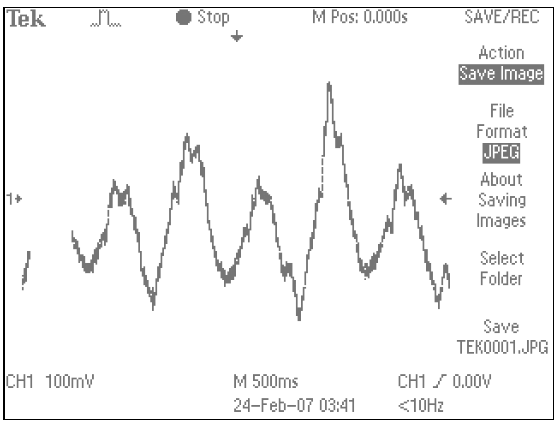

Figure 7: Oscilloscope screen shot of a pre-processed sample Common Carotid artery recording from a female subject.

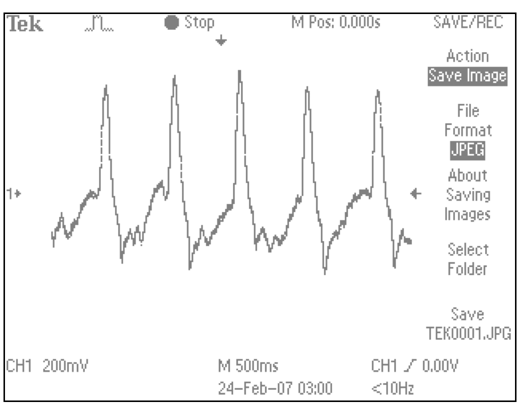

Figure 8: Oscilloscope screen shot of a pre-processed sample internal Carotid artery recording from a female subject.

4 PERLIMINARY TEST RESULTS

Using the radar system discussed in Section.2, the AMA signal was captured from a healthy female as shown in Figures. 7 to 9, for the Common Carotid artery, the internal Carotid artery and the Foramen spinosum of a female subject, respectively. These signals were captured in short recording duration, and should therefore be considered only preliminary at the moment.

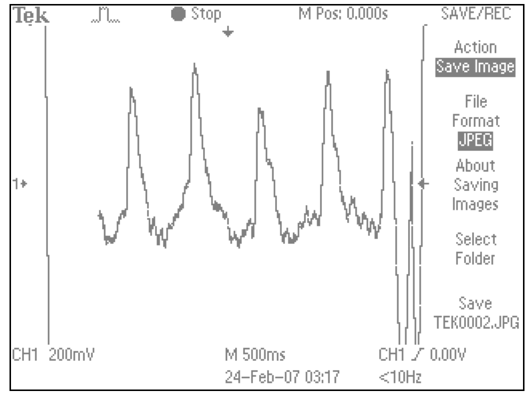

Figure 9: Oscilloscope screen shot of a pre-processed sample Foramen spinosum recording from a female subject.

5 CONCLUSION

In this paper, a Microwave Doppler-based radar system is used to measure heart-rate and blood flow in the Carotid arteries. Therefore, this system requires no physically connecting electrodes or other sensors to the body. A conceptual model and FDTD analysis confirm feasibility and reveal that most of the illuminating power is consumed in the skin. Finally, some preliminary short-time captured signals from the major arteries are depicted.

REFERENCES

[1]K.K. Shung, "Diagnostic Ultrasound: Imaging and Blood Flow Measurements," Francis Taylor: CRC Press, Boca Raton, FL, September, 2005.

[2]K. Tavakolian, F. Zadeh, Y. Chuo, A. Vaseghi, and B. Kaminska, "Development of a Novel Contactless Mechanocardiograph Device," J. Telemedicine and Applications, Article ID 436870, 2008.

[3]http://www.merck.com/mmpe/sec16/ch211/ch211a.html, Merck & Co. INC.

[4]Italian National Research Council, Institute of applied physics, Florence, Italy, http://niremf.ifac.cnr.it/tissprop/.

[5]D. M. Pozar, "Microwave Engineering," Wiley, 3rd Ed., New York, 2004.

[6]Federal Communications Commission (FCC) regulations, part 15.

[7]Avago Technologies, INC. HSMS282x Schottky diode series datasheet.

NSTI-Nanotech 2009, www.nsti.org, ISBN 978-1-4398-1783-4 Vol. 2, 2009